Received: 6 July 2021

DOI: 10.1002/mop.33069

WILEY

RESEARCH ARTICLE

Flexible-rate optoelectronic wireless transmission system at 101 GHz using multiband CAP-PAM modulation and envelope detection

Jiao Zhang[1,2] | Qinru Li[1] | Qingyi Zhou[1] | Min Zhu[1,2] | Shuang Gao[1] | Zilu Wang[1] | Bingchang Hua[2] | Yuancheng Cai[1,2] | Mingzheng Lei[2] | Liang Tian[2] | Yucong Zou[2] | Aijie Li[2]

[1]National Mobile Communications Research Laboratory, Southeast University, Nanjing, China

[2]Pervasive Communication Research Center, Purple Mountain Laboratories, Nanjing, China

Correspondence
Min Zhu, National Mobile Communications Research Laboratory, Southeast University, Nanjing 210096, China.
Email: minzhu@seu.edu.cn

Funding information
Research and Development, Grant/Award Number: BE2020012

Abstract

In this paper, we have experimentally demonstrated the first flexible-rate optoelectronic terahertz wireless transmission system at 101 GHz based on multiband CAP-PAM modulation and cost-efficient envelope detection. Instead of traditional M-QAM mapping, PAM-N mapping is used in CAP modulation with low-computational complexity. The system performances and optimal capacity in both single-band case and multiband case are intensively investigated. The results show that the highest data rate for single-band system is 13.35 Gbit/s with CAP-PAM-5 modulation, while the optimum aggregate transmission line rate of 8.49 Gbit/s can be obtained with 4-sub-bands CAP-PAM-{5,3,2,2} modulation under 7% FEC limit of 3.8×10^{-3} for four-user access.

KEYWORDS

envelope detection, intensity-modulation and direct-detection, optoelectronic wireless transmission, multiband carrier-less amplitude and phase modulation, multiuser access

1 | INTRODUCTION

With the rapid exhaustion of accessible transmission bands, the terahertz (0.1–10 THz) band with wider bandwidth and higher frequency has been attracting plentiful interests.[1,2] Photonics-aided wireless schemes based on intensity-modulation and direct-detection (IM/DD) have been broadly investigated,[3–6] which combine the flexibility of wireless communication, the broadband of optical fiber communication and lower complexity compared with coherent detection. Moreover, recent artificial intelligence-based optimization approaches, such as particle swarm optimization and ant colony[7] have been wildly utilized for designing electromagnetic and THz devices, including envelope detectors (ED),[8] phase correction,[9] and spatial filters,[10] which further promote the existing schemes.

Advanced modulation formats have also been proposed and widely employed to improve spectral efficiency. The IEEE P802.3bs 400 GbE Task Force adopted quaternary pulse amplitude modulation (PAM-4) as an industrial standard due to its simple DSP architecture and low-energy consumption.[11,12] The OFDM has been demonstrated to be an excellent modulation format due to its strong resilience to fiber chromatic dispersion (CD).[13,14] However, none of these formats mentioned can realize multiuser access with a simple IM/DD structure.

Recently, multiband carrier-less amplitude and phase modulation (CAP) has become a major candidate for multiuser access,[15,16] which has low-complexity of algorithm, simple structure, and flexibility of multiuser allocation. The multiband CAP-64 was employed in high-speed visible light communication (VLC) to implement a dynamic capacity for up to 9-user access.[17] A 56 Gbit/s multiband CAP signal transmission over 80-km single-mode fiber link is also experimentally demonstrated.[18] In these schemes, multiband CAP modulation with M-QAM mapping are used. To the best of our knowledge, there is no research on multiband CAP modulation using PAM-N mapping for the optoelectronic THz wireless transmission system.

In this paper, we proposed and experimentally demonstrated an envelope-detection-based THz wireless transmission system at 101GHz with multiband CAP-PAM modulation for the first time. Instead of traditional M-QAM mapping, PAM-N mapping is utilized in CAP modulation for low-computational complexity and easy implementation. At receiver, an ED is employed to achieve high-cost-efficient and low-structural complexity. We first investigated the bit error rate (BER) value versus the peak-to-peak voltage (V_{pp}) of baseband signal and the bias voltage (V_{bias}) of the intensity modulator (IM) in single-band cases. Based on the optimum parameters, the system performances and optimal capacity in both single-band case and multiband case are then intensively studied. The results show that the highest data rate for single-band system is 13.35 Gbit/s with 5.75 Gbaud PAM-5 modulation, while the optimum aggregate bit rate of 8.49 Gbit/s can be achieved for four-user access in multiband system with PAM-{5,3,2,2} modulation under 7% FEC limit of 3.8×10^{-3}.

2 | EXPERIMENTAL SETUP

The experimental setup of the optoelectronic THz wireless transmission system is shown in Figure 1. The baseband CAP-PAM signal is generated offline by MATLAB and uploaded into a 92GSa/s arbitrary waveform generator with 3-dB analog bandwidth of 32-GHz, and then amplified by a 20-GHz electrical amplifier (EA). The IM has a 3-dB bandwidth of 20-GHz. Two beams of continuous-wavelength light wave, with a 101 GHz frequency space, are generated by external cavity lasers ECL-1 and ECL-2, coupled by the optical coupler and then modulated in IM. After 1 km SSMF transmission, a variable optical attenuator is applied to adjust the received optical power for sensitivity measurement. Then, the baseband CAP-PAM signal is up-converted to a THz-wave signal at 101 GHz using a PD with 110-GHz bandwidth and amplified by a low-noise amplifier (LNA-1). A pair of W-band horn antennas are employed for 2-m wireless transmission. THz-wave signal received is amplified by another LNA-2, then recovered to baseband signal by an ED. The LNA at the transmitter and the receiver has a gain of 20 dB and 30 dB respectively, and both operating in the 80–110 GHz frequency range. Finally, the output signal is boosted via an EA and captured by a 33 GHz 80GSa/s real-time digital storage oscilloscope for further offline DSP.

For multiband CAP-PAM signals generation, the detailed transmitter offline DSP for each sub-band includes PRBS, PAM-N mapping, up-sampling, shaping filtering, resampling and normalization. The corresponding PRBS length of each band is 2^{13}–1. PAM-*N* signals with different levels are assigned according to the SNR in each sub-band. For receiver offline DSP, after a time synchronization, followed by the matched filtering, LMS and DD-LMS equalization, PAM-N de-mapping and BER calculation. LMS and DD-LMS equalization is implemented for inter carrier interference mitigation and precise decision, thus further improve the BER performance.

3 | EXPERIMENTAL RESULTS AND DISCUSSIONS

The system optimization is first performed in single-band cases. The influence of V_{bias} of the IM and V_{pp} of baseband CAP-PAM signal are investigated. Figure 2A depicts the results of V_{pp}, when the V_{bias} is set at 3.8 V. The roll-off factor of the filter is 0.1005. As shown in Figure 2A, the BER decreases with increased V_{pp} until an optimum value is achieved, and the optimum V_{pp} is approximately 200 mV. Then, the BER performance versus V_{bias} of the IM based on the optimum V_{pp} is shown in Figure 2B. The results show that there exists an optimum V_{bias} region of approximately 0.2 V (from 3.8 to 4.0 V) for PAM-5 and 0.6 V (from 3.6 to 4.2 V) for PAM-4. We comprehensively consider the performance of

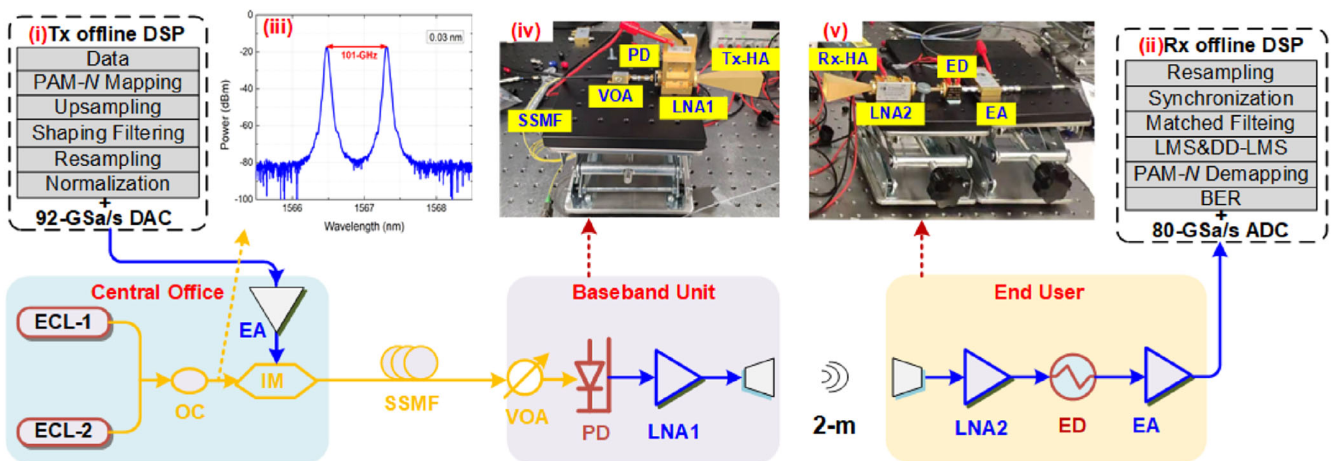

FIGURE 1 Experimental setup of the optoelectronic wireless transmission system with detailed DSP blocks. The specific experimental setup together with detailed offline DSP blocks at transmitter and receiver and their connection structure are shown in the figure. The inset figures (i) and (ii) are detailed structure of offline DSP blocks at transmitter and receiver, (iii) is the optical spectrum after OC, and (iv) and (v) are the pictures of the actual structure of the baseband unit and end user. The abbreviations of devices are interpreted as follows: ECL-1,2, external cavity laser; OC, optical coupler; IM, intensity modulator; EA, electrical amplifier; LNA-1, 2, low-noise amplifier; VOA, variable optical attenuator; SSMF, standard single mode fiber; PD, photonic detector; ED, envelop detector. The blue line in the figure represents the electrical signal and the yellow line represents the optical signal

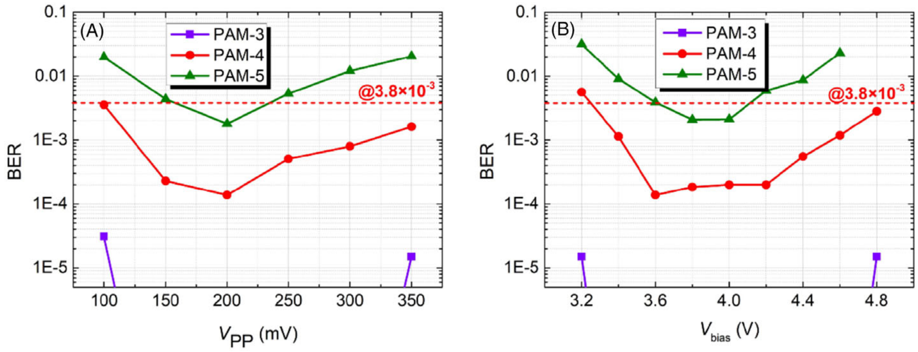

FIGURE 2 The BER performances versus (A) Vpp of CAP-PAM baseband signals; (B) Vbias of the IM. The BER performance versus the Vpp of CAP-PAM baseband signals is shown in Figure 2A and the BER performance versus the Vbias of the IM is shown in the Figure 2B. The red dotted line is the 7% FEC limit of 3.8×10^{-3}. The line with triangles represents the single-band CAP-PAM-3 signal, the line with circles represents the single-band CAP-PAM-4 signal, and the line with squares represents the single-band CAP-PAM-5 signal

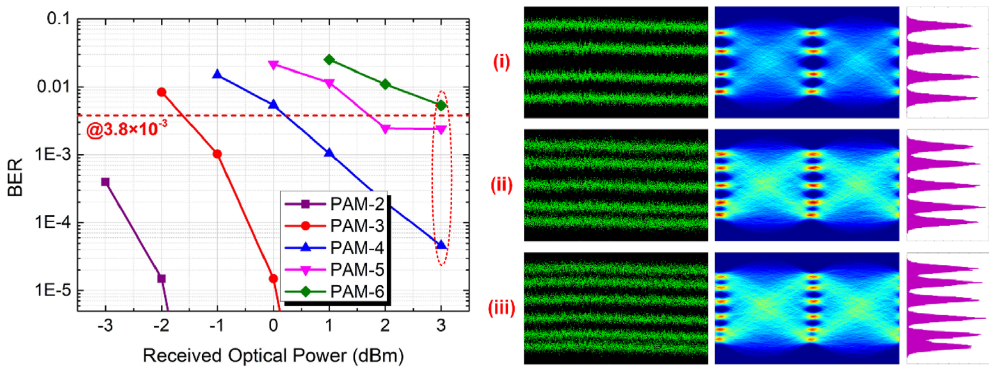

FIGURE 3 The BER performances versus different ROP for 5.75 GBaud CAP-PAM-{2,3,4,5,6} signals. The BER performances versus different ROP for CAP-PAM-{2,3,4,5,6} signals at the symbol rate of 5.75 GBaud/s is shown on the left. The red dotted line is the 7% FEC limit of 3.8×10^{-3}. The color of the line for CAP-PAM-{2,3,4,5,6} signals is purple, red, blue, pink and green, respectively. The recovered symbols, eye diagrams and histograms for PAM-{4,5,6} at 3 dBm ROP are shown on the right (i)–(iii)

different PAM levels, the optimal value for V_{bias} and V_{pp} are set at 3.8 V and 200 mV, respectively.

Based on the optimized V_{pp} and V_{bias} parameters, we then assess the transmission performance of the single-band case. Figure 3 shows the specific BER performances versus different ROP for 5.75 GBaud single-band CAP-PAM-{2,3,4,5,6} signals. The sensitivity is defined as the minimum acceptable value of the ROP with BER of 3.8×10^{-3}. It can be observed that the BER performances deteriorates with increased modulation order and reduced the ROP. Compared to the CAP-PAM-3 signal, the CAP-PAM-4 signal and CAP-PAM-5 signal suffer 1.9 dB and 3.4 dB of penalty in the sensitivity, respectively. The worst performance occurs for the CAP-PAM-6 signal, which fails to meet the BER target because higher order symbols are more susceptible to nonlinear impairment. As a result, the highest baud rate achieved in single-band cases is 13.35 Gbit/s with PAM-5 modulation. Insets (i)–(iii) are recovered symbols, eye diagrams and histograms for PAM-{4,5,6} at 3-dBm ROP, respectively.

Furthermore, the electrical spectra of CAP-PAM signals at transmitter and receiver are shown in Figure 4, respectively. The center frequency of single-band signal is set at 3.81625 GHz with a total bandwidth of 5.75 GHz. It can be seen that both single-band signal and multiband signal suffer an attenuation in high-frequency components. What's more, the single-band CAP-PAM signal shows strong side lobes, which can be significantly suppressed in multiband case because signal is divided into smaller sub-bands. In this experiment, a multiband CAP-PAM signal with four sub-bands is successfully transmitted. The four sub-bands are located on the different center frequency of 0.791 GHz, 2.516 GHz, 4.241 GHz and 5.966 GHz with a total bandwidth of 5.75 GHz. The multiband CAP-PAM signals are optimized with the appropriate PAM level for each sub-band, which employed PAM-5 for the first band, PAM-3 for the second band and PAM-2 for the last two bands.

Finally, the BER performances versus different ROP for each sub-band are presented in Figure 5. As we can observe, the transmission performances of all the four sub-bands can

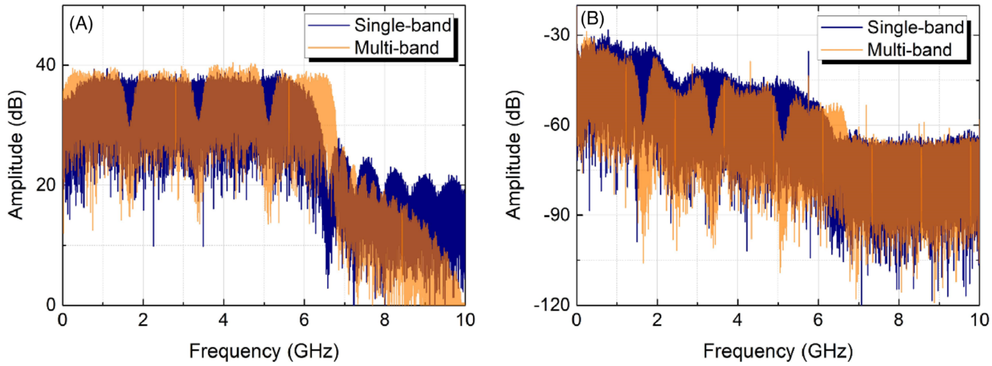

FIGURE 4 The spectra of CAP-PAM signals (A) At transmitter, (B) At receiver. The spectrum of CAP-PAM signals at transmitter is shown in Figure 4A and the spectrum of CAP-PAM signals at receiver is shown in Figure 4B. The blue one is the single-band signal and the yellow one is the multiband signal

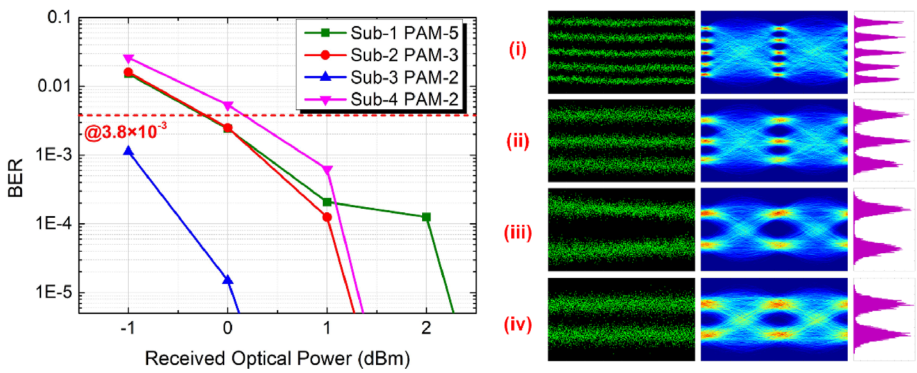

FIGURE 5 The BER performances versus different ROP for each sub-band. The BER performances versus different ROP for each sub-band in multiband case is show on the left. The red dotted line is the 7% FEC limit of 3.8×10^{-3}. The color of the line for sub-{1,2,3,4} is green, red, blue and pink, respectively. The recovered symbols, eye diagrams and histograms for 4-sub-bands at 3.8 × 10–3 limit with PAM-{5,3,2,2} are shown on the right (i)–(iii)

meet the 7% FEC limit of 3.8×10^{-3} with the ROP above 0.2 dBm. The sub-1 and sub-2 show similar performances with the ROP under 1 dBm, while the sub-4 suffers a 0.5 dBm of penalty. Meanwhile, the sub-3 has the best performance due to selection of PAM-2 at the cost of a lower transmission capacity. Figure 5(i)–(iv) are recovered symbols, eye diagrams and histograms for 4 sub-bands at 3.8×10^{-3} limit. In this demonstration, the aggregate data rate of the multiband CAP-PAM system is 8.49 Gbit/s.

According to the experimental results, the baud rate degrades in multiband system compared to single-band system, which is the major limitations of present research. The decreasing of system capacity can be explained for several reasons. First, several independent sub-bands may lead to a higher peak to average power ratio, which causes worse system performance. Meanwhile, with the increasing of sub-bands, the average SNR of the high-index sub-band will degrade due to sever high-frequency attenuation, thus those sub-bands with poor BER performance significantly limit the performance of the overall system. Finally, the inherent bandwidth limitation of the traditional ED is the greatest obstacle. In this respect, optimized devices designed through nature-based algorithms as mentioned before can be utilized for further increase of system capacity and thus may become the direction of future research.

4 | CONCLUSIONS

In conclusion, the first flexible-rate optoelectronic wireless transmission system at 0.1-THz based on multiband CAP-PAM modulation and envelope detection was experimentally demonstrated. PAM-N mapping is utilized instead of traditional M-QAM mapping in CAP modulation for low-computational complexity, low cost and easy implementation. Meanwhile, an ED is employed to further realize high-cost-efficient. The measured results show that the highest bit rate achieved for the single-band system is 13.35 Gbit/s with PAM-5 modulation. By using the multiband CAP-PAM modulation, a dynamic capacity can be achieved for 4-sub-bands, and the aggregate transmission rate of 8.49 Gbit/s can be successfully achieved with the BER under 3.8×10^{-3} for four-user access. From the above, CAP-PAM modulation and envelope detection may be the appropriate choice for optoelectronic THz wireless system considering higher cost efficiency, flexible transmission rate, and multi-user access.

ACKNOWLEDGMENT

This work was supported in part by the Key Research and Development Program of Jiangsu Province under Grant BE2020012, and the Transformation Program of Scientic and Technological Achievements of Jiangsu Province under Grant BA2019026 (Jiao Zhang and Qinru Li contributed equally to this work).

DATA AVAILABILITY STATEMENT

The data that support the findings of this study are available from the corresponding author upon reasonable request.

REFERENCES

[1] Ullah S, Ullah R, Zhang Q, et al. Ultra-Wide and Flattened Optical Frequency Comb Generation Based on Cascaded Phase Modulator and LiNbO3-MZM Offering Terahertz Bandwidth. *IEEE Access*. 2020;8:76692-76699. doi:10.1109/ACCESS.2020.2989678

[2] Yu J. Large-Capacity Optical and Wireless Seamless Integration and Real-Time Transmission System. *Broadband Terahertz Commun Technol*. Singapore: Springer; 2021;245-264. doi:10.1007/978-981-16-3160-3_12

[3] Moon S et al. Demonstration of photonics-aided terahertz wireless transmission system with using silicon photonics circuit. *Opt Express*. 2020;28(16):23397-23408. doi:10.1364/OE.398460

[4] Nagatsuma T. Advances in terahertz communications accelerated by photonics technologies. *Proc. 24th OptoElectron Commun Conf Int Conf Photon Switching Comput*. 2019;1-3. doi:10.23919/PS.2019.8818026

[5] Ullah R, Ullah S, Ali A et al. Optical 1.56 Tbps coherent 4-QAM transmission across 60 km SSMF employing OFC scheme. *AEU-Int J Electron Commun*. 2019;105:78-84.

[6] Ullah R, Ullah S, Khan GZ, et al. Ultrawide and tunable self-oscillating optical frequency comb generator based on an opto-electronic oscillator. *Results Phys*. 2021;22:103849. doi:10.1016/j.rinp.2021.103849

[7] Pooia L, Bahram Z, Ali L. An Improved Model of Ant Colony Optimization Using a Novel Pheromone Update Strategy. *IEICE T Inf Syst*. 2013;E96-D(11):2309-2318. doi:10.1587/transinf.E96.D.2309

[8] Tyagi S, Panigrahi SK. An improved envelope detection method using particle swarm optimisation for rolling element bearing fault diagnosis. *J Comput Des Eng*. 2017;4(4):305-317. doi:10.1016/j.jcde.2017.05.002

[9] Lalbakhsh A, Afzal MU, Zeb BA & Esselle KP Design of a dielectric phase-correcting structure for an EBG resonator antenna using particle swarm optimization. IEEE Conf Int Sym Ant Prop (ISAP). 2015;1-3.

[10] Lalbakhsh A, Esselle KP. Directivity improvement of a Fabry-Perot cavity antenna by enhancing near field characteristic. *17th IEEE Int. Sym. Ant. Technol. Applied Electrom. (ANTEM)*. 2016; 1-2. doi:10.1109/ANTEM.2016.7550182

[11] Zhang J, Yu J, Li X, et al. 100 Gbit/s VSB-PAM-n IM/DD transmission system based on 10 GHz DML with optical filtering and joint nonlinear equalization. *Opt Express*. 2019;27(5):6098-6105. doi:10.1364/OE.27.006098

[12] Zhang J, Xin X, Zhao F, et al. SOA pre-amplified 100 Gb/s/λ PAM-4 TDM-PON downstream transmission using 10 Gbps O-band transmitters. *J LightwTechnol*. 2020;38(2):185-193. doi:10.1109/JLT.2019.2944558

[13] Boulogeorgos AAA, Papasotiriou E, Alexiou A. A distance and bandwidth dependent adaptive modulation scheme for THz communications. *Proc. 19th IEEE Int Workshop Signal Process Adv.Wireless Commun (SPAWC)*. 2018;1-5. doi:10.1109/SPAWC.2018.8445864

[14] He J, Long F, Deng R, Shi J, Dai M, Chen L. Flexible multiband OFDM ultra-wideband services based on optical frequency combs. *JOpt Commun Netw*. 2017;9(5):393-400. doi:10.1364/JOCN.9.000393

[15] Wei J, Giacoumidis E. Multi-band CAP for next-generation optical access networks using 10-G optics. *J Lightw Technol*. 2018; 36(2):551-559. doi:10.1109/JLT.2017.2772894

[16] Werfli K, Chvojka P, Ghassemlooy Z, et al. Experimental demonstration of high-speed 4×4 imaging multi-CAP MIMO visible light communications. *J. Lightw. Technol.* 2018;36(10):1944-1951. doi:10.1109/JLT.2018.2796503

[17] Wang Y, Tao L, Wang Y, Chi N. High speed WDM VLC system based on multi-band CAP64 with weighted pre-equalization and modified CMMA based post-equalization. *IEEE Commun Lett*. 2014;18(10):1719-1722. doi:10.1109/LCOMM.2014.2349990

[18] Wei J, Eiselt N, Sanchez C, Du R, Griesser H. 56 Gbit/s multi-band CAP for data center interconnects up to an 80 km SMF. *Opt Lett*. 2016;42(17):4122-4125. doi:10.1364/OL.41.004122

How to cite this article: Zhang J, Li Q, Zhou Q, et al. Flexible-rate optoelectronic wireless transmission system at 101 GHz using multiband CAP-PAM modulation and envelope detection. *Microw Opt Technol Lett*. 2022;64:208–212. https://doi.org/10.1002/mop.33069